The arrival time distribution near the EAS core at Taro

N.SUZUKI[1], M.FUKUOKA[1],H.KURAMOCHI[2], H.SAKUYAMA[1],NOBORU.SUZUKI[1]
[1]*Department of Physics, Meisei university, Tokyo 191-8506, Japan*
[2] *Adoc International Co.,Ltd, Tokyo 190-0012, Japan*
06m1005@phys.meisei-u.ac.jp

Abstract: The arrival time distriution of EAS has been observed by using Ultra Fast Cherenkov detectors(UFC) and new Fast Scintillation(FS) detectors at Taro (200m a.s.l.). The main EAS array consists of 169 $0.25m^2$ and 100 $0.0225m^2$ scintillation detectors in a lattice configuration. The other 40 $1m^2$ and $0.25m^2$ scintillation detectors are arranged up to $100m$ from the center of the array. FS detectors are placed at $11 \sim 14m$ from the center of the lattice array. The EAS array was triggered by three fold coincidence of three fast scintillation detectors placed at the central part of the lattice array. The accuracy of the measured distance between core axis and the FS detectors was estimated as precisely. We report the results of rise time, FWHM and fall time near the EAS core in a various EAS size range.

Introduction

After the report [1], we set up 4 new FS detectors at Taro cosmic ray laboratory(Fig4,Fig5). Fast timing plastic scintillator BC-420, fast photomultiplier tube that was made by Hamamatsu including R2083 of Meisei university specification, and high frequency coaxial cable were used for these FS detectors. Each table 1,2,3 show detailed these parts properties.

Analysis

To examine Tr,Tf, and FWHM[1] of the FS detector in a various EAS size, we decided EAS size. We used the data obtained from observation period : August 6, 2005 $\sim$ June 12, 2006 as following conditions.

1. There is the detector recorded maximum particle in a TASC-1(Fig4) .
2. EAS size(Ne) is more than 10^4.
3. Pluse height of FS detector is more than 50mV and the signal does not overflow on the oscilloscope.
4. FWHM is more than 2ns.

Condition 4 was performed in order to exclude the influence of the PMT pluse[1].

Rsults and discussions

Table 4 shows the analyzed event count in each size of FS detector and table 5 shows relation between class and size. FWHM and Tf show a tendency to increase slightly as N_e increases(Fig1). Moreover, to remove the dependence of the distance from the EAS core to the FS detector, we picked up events of same distance(=r) from the EAS core to the FS detector and analyzed it again. But the tendency hardly change(Fig2).

References

[1] N.Suzuki et al.,Proc. 29th ICRC Pune,HE1.5.(2005)

1. We define the duration from 50% to 50% of ph(pluse height) as FWHM, from 10% to 90% of ph as Tr, and 90% to 30% of ph as Tf.

Physical Properties	
Density	1.032 g/cm^3
Refractive index	1.58
Coefficient of thermal expansion	0.0078 $\%/°$C
Rise Time	0.5[ns]
Decay Time	1.5[ns]

Table 1: Plastic Scintillator (Bicron BC-420)

Spectral response	300 to 650[nm]
dynode(number of stages)	8
Gain	2.50×10^6
Rise time	0.7[ns]
Voltage	-3000[V]

Table 2: PMT (Hamamatsu R2083 H2431-50)

Type	Attenuation (dB/km)	
100-SFA	430MHz	900MHz
	59	92

Table 3: Signal Cable (High-frequancy coaxial cable)

	Class1	Class2	Class3	Class4	Class5	Class6	Class7	Class8	Total
FS3	135	1040	3259	1713	809	365	47	4	7372
FS4	30	319	1394	990	598	351	51	9	3742
FS5	6	164	900	560	395	283	55	9	2372
FS6	29	417	1638	879	532	341	53	8	3897

Table 4: Number of events in each FS detector

Class	Size
Class1	$1.0 \times 10^4 \leq Ne < 2.2 \times 10^4$
Class2	$2.2 \times 10^4 \leq Ne < 4.6 \times 10^4$
Class3	$4.6 \times 10^4 \leq Ne < 1.0 \times 10^5$
Class4	$1.0 \times 10^5 \leq Ne < 2.2 \times 10^5$
Class5	$2.2 \times 10^5 \leq Ne < 4.6 \times 10^5$
Class6	$4.6 \times 10^5 \leq Ne < 1.0 \times 10^6$
Class7	$1.0 \times 10^6 \leq Ne < 2.2 \times 10^6$
Class8	$2.2 \times 10^6 \leq Ne < 4.6 \times 10^6$

Table 5: Relation between Class and Size(Ne)

ICRC 2007 Proceedings - Pre-Conference Edition

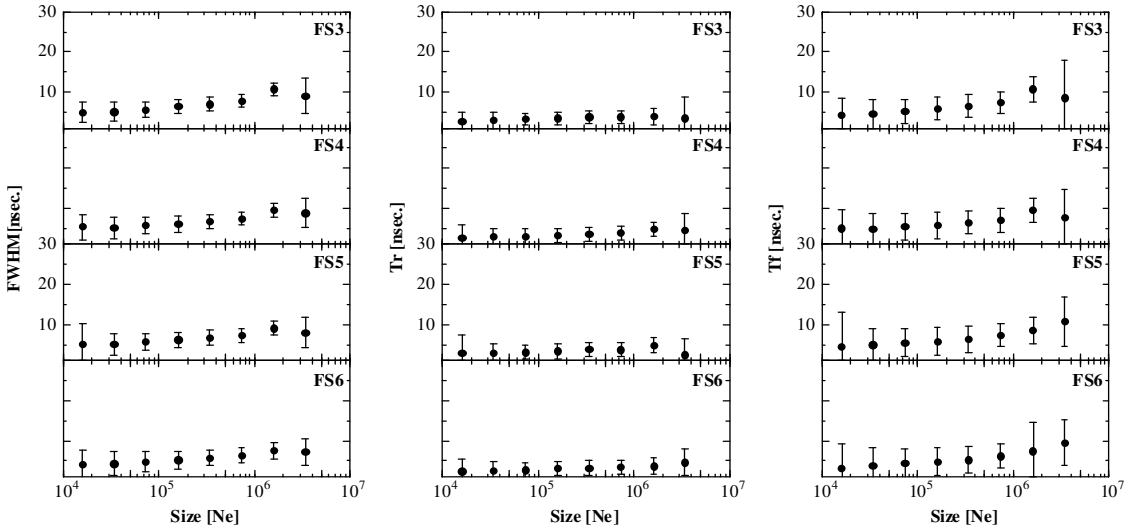

Figure 1: Relation between EAS size and FWHM,Tr,Tf

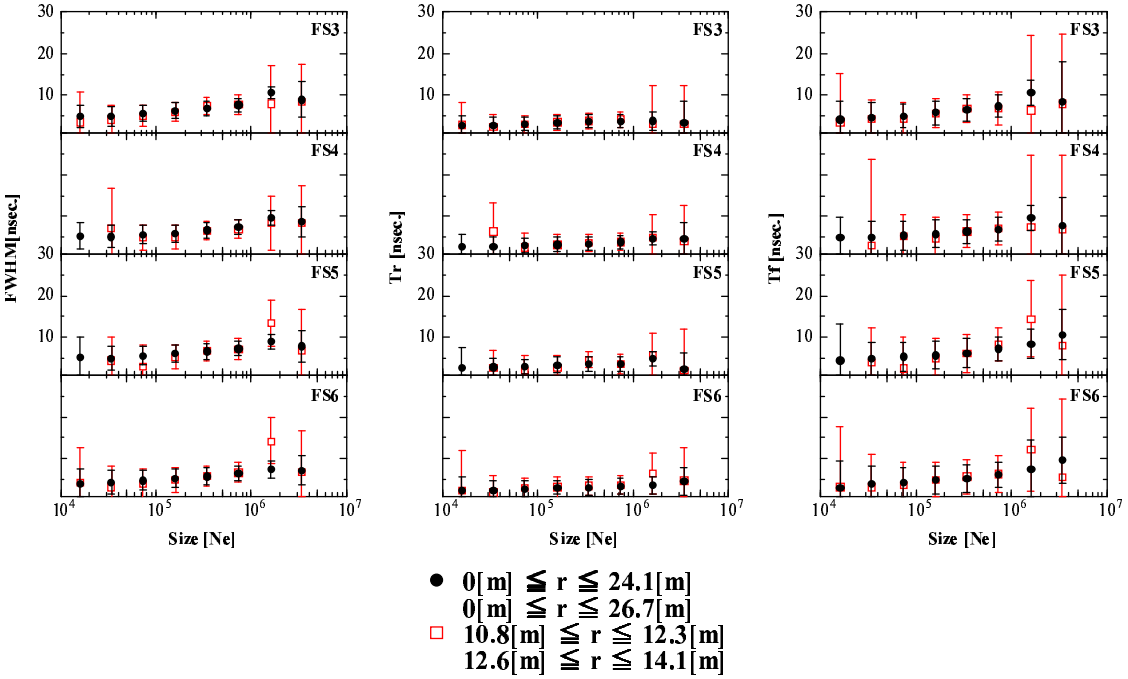

Figure 2: Relation between EAS size and FWHM,Tr,Tf

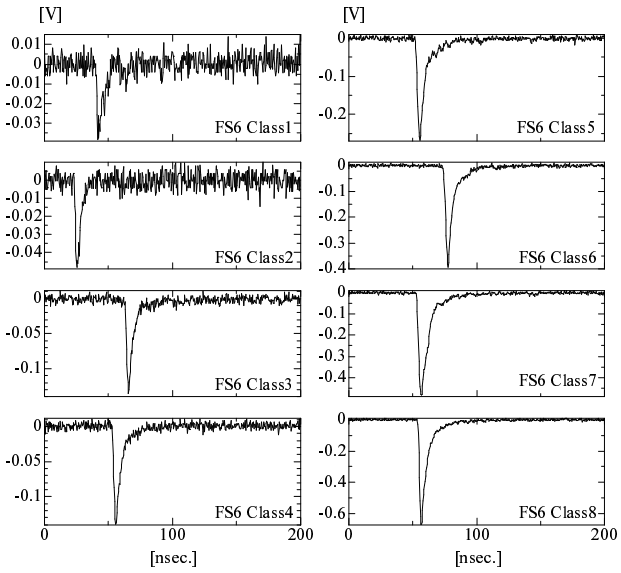

Figure 3: Example of waveforms on FS6 detector in each class

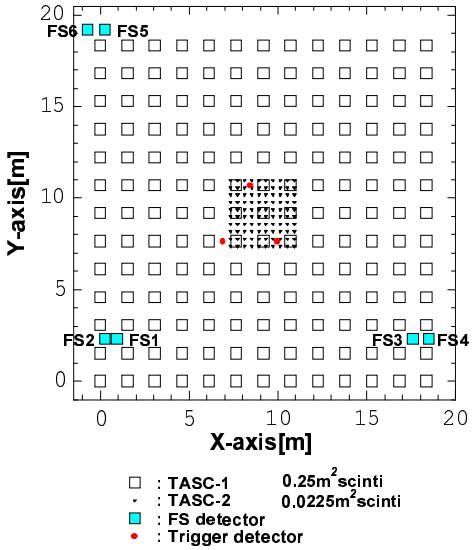

Figure 4: Arrangement of Core detector

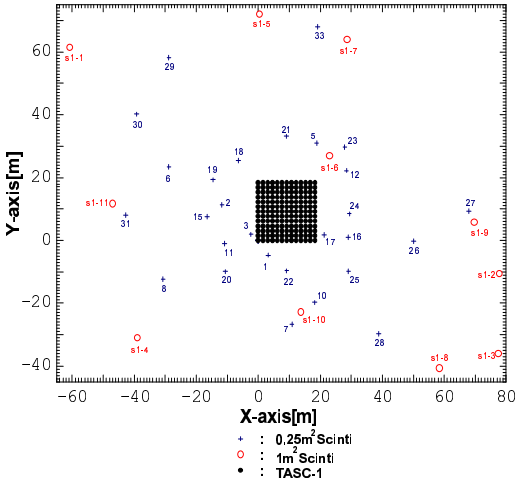

Figure 5: EAS array

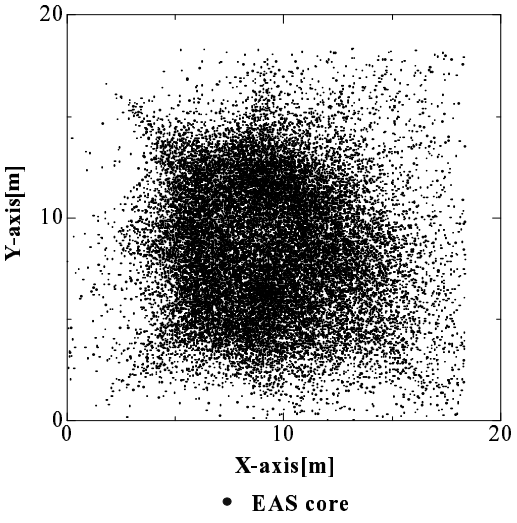

Figure 6: Distribution of EAS core in TASC-1